HE397
The Standard Model of Particle Physics
Electroweak Precision Measurements

Sudipta Mondal (SR 24632)
Rahul Agarwal Singh (SR 22246)
Chaitanya Bhatt (SR 17073)

April 01, 2025

1 Introduction

The Standard Model (SM) of particle physics is a well-established theory that describes the electromagnetic, weak, and strong interactions. However, it is known to be incomplete, as it does not incorporate gravity and does not explain certain phenomena such as dark matter and neutrino masses. The search for physics beyond the Standard Model (BSM) is an active area of research, and one of the key approaches to probe BSM physics is through electroweak precision measurements (EWPMs). These measurements are sensitive to virtual effects of new particles and interactions that may exist at energy scales beyond the reach of current colliders.

EWPMs allowed precise measurements of gauge coupling constants, that seemed to suggest their unification within SUSY extension of the SM and increased interest in SUSY and GUTs, and advent of interesting theories like radiative electroweak symmetry breaking that predict uniqueness of the Higgs mechanism as a mass-providing mechanism. We are familiar with the consequences of one-loop corrections in QED and in non-Abelian gauge theories with simple gauge groups, like QCD. What about the Standard Model (in particular, the electroweak sector)?

Loop contributions in the Standard Model pave the way for EWPMs: they allow precise tests of the Standard Model as well as help probe BSM physics. Clearly, one-loop diagrams would lead to more precise predictions than tree-level-ones.

But *a priori*, we would expect an unmanageable number of them. We need to systematize our approach, organize one-loop contributions, and filter out the ones which would not be susceptible to current experiments. This is the programme of EWPMs.

In the pure electroweak sector, at tree-level, we have only three independent parameters: the couplings g and g', and the VEV of the Higgs field, v. Alternatively, we can work with the following:

1. The fine structure constant,

$$\alpha = \frac{g^2}{4\pi} \sin^2 \theta_W,$$

measured from the Quantum hall effect and g-2 of the electron,

2. The Z-boson mass,

$$m_Z^2 = \frac{1}{4}(g^2 + g'^2)v^2,$$

obtained from direct measurements of Z-decay width,

3. The Fermi constant,

$$G_F = \frac{1}{\sqrt{2}v^2},$$

obtained from muon decay.

These parameters are more accurately measurable than g, g' and v. There are more observable quantities than there are parameters in the electroweak sector; clearly this imposes relations between the observables, *at tree-level*.

At loop-level, the number of parameters is no longer just 3; the rest of the Standard Model will interfere. Thus, *tree-level relations between observables will be violated*.

These relations will also be violated by violation of symmetries (e.g. $SU(2)$ custodial symmetry[1]) of the electroweak sector that are not respected by the full Standard Model, as well as non-renormalizable terms coming from BSM (Beyond the Standard Model) physics. EWPMs are tests of tree-level relations expected to be violated at loop-level. They allow testing the Standard Model more precisely, and help us look for BSM effects. We classify EWPMs into high-energy and low-energy processes:

- Low-energy processes are ones where the energy scale of the process is well below the W and Z masses; W and Z bosons are way off-shell. Examples: neutrino scattering, deep inelastic scattering, atomic parity violation, low-energy e^-e^+ scattering, etc.
- High-energy processes are ones where either W or Z is on-shell. Examples: measurements of W, Z masses and their partial and total decay widths, etc.

2 Physical observables

2.1 Discrepancy in the definition of θ_W

First, we take a detour, and present a discrepancy in the measured weak mixing angle.

On the one hand, the angle θ_W can be measured from the W mass and the relation

$$M_W^2 = \frac{\pi\alpha}{\sqrt{2}G_F \sin^2\theta_W}$$

This measured value turns out to be[2]

$$\sin^2\theta_W = 0.215 \pm 0.002.$$

[1] of the Higgs potential, not the full EW sector

[2] J. Alitti et al., UA2 Collaboration, Phys. Lett. B **276**, 354 (1992).

On the other hand, measurements from quark couplings gives[3]

$$\sin^2\theta_W = 0.233 \pm 0.003(exp.) \pm 0.005(theo.)!$$

The discrepancy is resolved as follows: first note that 'the' weak mixing angle θ_W is defined by

$$\tan\theta_W = \frac{g'}{g}.$$

There are 3 quantities that are equal to this θ_W at tree-level, but must differ from it at loop-level. We call them 'weak mixing angles' as well, and denote them, here, by θ_0, θ_W and θ_*^f. We define them below, and these will be our 'high-energy observables'. Some of these angles are defined as follows:

$$sin^2\theta_0 = \frac{\pi\alpha}{\sqrt{2}G_F m_W^2},$$
$$\sin^2\theta_W = 1 - \frac{m_W^2}{m_Z^2}$$
$$\implies \rho_0 \equiv \frac{m_W^2}{m_Z^2\cos^2\theta_W} = 1 \text{ at tree level}$$

and, finally, motivated from the tree-level relation $g_V^f = T_3^{f,R} + T_3^{f,L} - 2Q^f\sin^2\theta_W$,

$$\sin^2\theta_*^f = \frac{T_3^{f,L} - g_V^f}{2Q^f}.$$

There is one θ_*^f for each charged fermion f, so there are 9 of these in the Standard Model.

Now, we analyze the loop corrections to θ_W.

$$A = \sqrt{\frac{\pi\alpha}{\sqrt{2}G_F}} \approx 37.28038(1)\ GeV,$$

we get, in the on-shell renormalization scheme,

$$\sin^2\theta_W = \frac{\frac{A^2}{M_W^2}}{1-\Delta r}$$

where
$\Delta r \equiv \Delta r_0 - \rho_t/\tan^2\theta_W$ is the loop contribution to θ_W,
$\Delta r_0 = 1 - \frac{\alpha}{\alpha(M_Z)} \approx 0.06630(7)$, and
$\rho_t = \frac{3G_F m_t^2}{8\sqrt{2}\pi^2} \approx 0.00936\left(\frac{m_t}{172.83\ GeV}\right)^2$

[3] J. V. Allaby et al., CHARM Collaboration, Z. Phys. C **36**, 611 (1987); A. Blondel et al., CDHS Collaboration, Z. Phys. C **45**, 361 (1990).

Some definitions

$$\begin{aligned} g_V^f &= g_L^f + g_R^f = \sqrt{\rho_f}(T_3^f - 2Q^f \sin^2\theta_*) \\ g_A^f &= g_L^f - g_R^f = \sqrt{\rho_f} T_3^f \\ \sin^2\theta_*^f &= \kappa^f \sin^2\theta_W \end{aligned}$$

At tree level, we have $\rho_f = \rho_0 \equiv 1$, except for the b-quark, due to the vertex correction from a triangle loop with top quarks and a W boson.

$$\rho_b \approx 1 + \frac{4}{3}\rho_t,\ \kappa_b \approx 1 + \frac{2}{3}\rho_t$$

$\sin^2\theta_*$ has been measured by EWWG at LEP.

2.2 Low Energy EW observables and Michel parameters

Low-energy observables come from neutrino scattering: $\bar{\nu}_l l \to \bar{\nu}_{l'} l'$.

In a general theory, the amplitude for such a process would be

$$\mathcal{M} = \frac{4G_F}{\sqrt{2}} \sum_{\gamma=S,V,T;\ \lambda,\mu=L,R} g_{\lambda\mu}^{\gamma} [\bar{l}_\lambda \Gamma_\gamma \nu_l][\bar{\nu}_l \Gamma^\gamma l_\lambda]$$

where
γ is the current type (scalar, vector or tensor), and λ, μ describe the chirality (left- or right-handedness).

From these $g_{\lambda\nu}^{\gamma}$, we can construct transition probabilities Q_{LR}, and, in turn, observables.

As an example, for the specific case of $l \to \nu_l e \bar{\nu}_e$, we have the cross section

$$\begin{aligned} \frac{d\Gamma}{dx d\Omega} = \frac{G^2 m_l^5}{192\pi^4} x^2 \Bigg\{ & 3(1-x) + \frac{2}{3}\rho(4x-3) + 6\eta \frac{m_e}{m_l}\frac{1-x}{x} \\ & \pm \xi P_l \cdot cos\theta [1 - x + \frac{2}{3}\delta(4x-3)] \Bigg\} + O\left(\left(\frac{m_e}{m_l}\right)^2\right) \end{aligned}$$

where
$x = \frac{E_e}{E_l}$, P_l = lepton polarization, θ = angle between electron momentum and lepton polarization, and ρ, η, ξ, δ are functions of the $g_{\lambda\mu}^{\gamma}$, known as *Michel parameters*.
Michel parameters are *observables* and the Standard Model predicts

$$\begin{aligned} \rho &= \delta = 3/4 \\ \xi &= 1 \\ \eta &= 0. \end{aligned}$$

Deviations of measured values from the above would imply violation of the SM.

2.3 Counting relevant parameters

- Excluding θ_{QCD}, and the neutrino mixing angles (PMNS matrix), the full SM has 18 parameters.
- Outside the electroweak sector, there are 15 parameters, of which 8 Yukawa couplings (for leptons and all quarks except t), and 3 CKM angles are too small to have noticeable tree-level-deviation effects.
- The CKM phase δ has negligible effect on flavour-diagonal processes.
  α_s has negligible effect as well, because gluons do not directly couple to W and Z, and α_s is flavour-universal.
- **The only important parameters that remain are: the top mass m_t and the Higgs mass m_H.**

Hence, all tree-level-deviations to the mixing angles will mostly come from 2 parameters only. This reduces the complexity of EWPMs significantly.

2.4 Oblique corrections

The only deviations from tree-level that will matter are those that come from corrections to the gauge boson propagators. Therefore, we can set all θ_*^fs equal.

Further, we ignore contributions from quarks lighter than b.

Oblique-corrected propagators are given by:

$$P_{AB} = \frac{-i}{q^2 - m_A^2}\left[\delta_{AB} + \frac{-i\Pi_{AB}(q^2)}{q^2 - m_B^2}\right]$$

By charge conservation, only Π_{WW}, Π_{ZZ}, $\Pi_{\gamma\gamma}$ and $\Pi_{\gamma Z}$ will be nonzero.
By gauge-invariance, $\Pi_{\gamma\gamma}(q^2 = 0) = \Pi_{\gamma Z}(q^2 = 0) = 0$

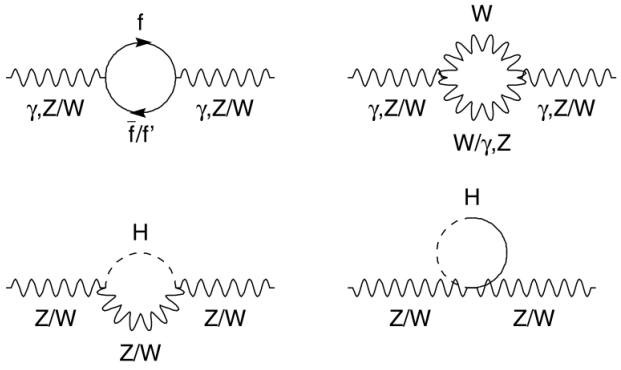

Figure 1: Examples of one-loop corrections to gauge boson propagators

- For low-energy EWPMs ($q^2 << M_W^2$), we can expand the propagators as follows:

$$\Pi_{AB}(q^2) = \Pi_{AB}(0) + q^2\Pi'_{AB}(0) + O((q^2)^2)$$

- High-energy EWPMs depend on $\Pi_{WW}(m_W^2)$, $\Pi_{ZZ}(m_Z^2)$ and $\Pi_{\gamma Z}(m_Z^2)$.

Hence, four functions are reduced to nine numbers. In terms of these numbers,

$$\begin{aligned}\sin^2\theta_0 - \sin^2\theta_* &= \frac{\sin^2 2\theta}{4\cos 2\theta}\left[\Pi'_{\gamma\gamma}(0) + \frac{\Pi_{WW}(0)}{m_W^2} - \frac{\Pi_{ZZ}(m_Z^2)}{m_Z^2}\right] \\ &\quad + \sin\theta\cos\theta\frac{\Pi_{\gamma Z}(m_Z^2)}{m_Z^2}, \\ \sin^2\theta_W - \sin^2\theta_* &= -\frac{1}{m_Z^2}\left[\Pi_{WW}(m_W^2) - \frac{m_W^2}{m_Z^2}\Pi_{ZZ}(m_Z^2)\right] \\ &\quad + \sin\theta\cos\theta\frac{\Pi_{\gamma Z}(m_Z^2)}{m_Z^2}\end{aligned}$$

From the above relations, it is possible to show that:

$$\begin{aligned}\sin^2\theta_0 - \sin^2\theta_* &= \frac{3\alpha}{16\pi\cos^2 2\theta}\frac{m_t^2 - m_b^2}{m_Z^2}, \\ \sin^2\theta_W - \sin^2\theta_* &= \frac{-3\alpha}{16\pi\sin^2\theta}\frac{m_t^2 - m_b^2}{m_Z^2}.\end{aligned}$$

- BEFORE direct measurements of the top and Higgs mass, EWPMs were used to measure these masses indirectly.
- AFTER direct measurements of these masses, EWPMs can be used to check the consistency of the SM.

Measuring the above θ's provides an indirect measurement of m_t^2.

Note 1: The factor $m_t^2 - m_b^2$ is the largest custodial-symmetry-breaking parameter within the SM.
Note 2: The decoupling theorem *appears* to be violated here.
Note 3: The relations are less sensitive to M_H than m_t because one loop corrections are logarithmically proportional to M_H due to the screening theorem.

3 Probing BSM using EWPMs

3.1 Probing BSM physics: S, T and U

We consider possible SMEFTs (SM Effective Field Theories). This is just the SM with additional non-renormalizable operators, that have little effect at $q^2 << \Lambda^2$, where $\Lambda >> m_W$ is some high BSM scale.

We ignore effects from new, heavy BSM gauge bosons, and loop-level BSM effects.

The lowest dimensional nonrenormalizable terms we consider are dimension-6, containing only electroweak gauge bosons and the Higgs. The nonrenormalizable Lagrangian is

$$\mathcal{L}_{nr} = \frac{1}{\Lambda^2}(c_{WB}O_{WB} + c_{HH}O_{HH} + c_{BB}O_{BB} + c_{WW}O_{WW})$$

where

$$\begin{aligned}
O_{WB} &= H^\dagger \tau^a H W^a_{\mu\nu} B_{\mu\nu} \to \frac{1}{2} v^2 W^3_{\mu\nu} B_{\mu\nu} \\
O_{HH} &= |H^\dagger D_\mu H|^2 \to \frac{1}{16} v^4 (g W^3_\mu - g' B_{mu})^2 \\
O_{BB} &= (\partial_\rho B_{\mu\nu})^2 \\
O_{WW} &= (D_\rho W^a_{\mu\nu})^2
\end{aligned}$$

The 'full' SMEFT Lagrangian is

$$\mathcal{L} = \mathcal{L}_{SM} + \frac{1}{\Lambda^2}\mathcal{L}|_{d=6} + \frac{1}{\Lambda^4}\mathcal{L}|_{d=8} + \cdots$$

We truncate our propagators to $O((q^2)^2)$ and $O(1/\Lambda^2)$:

$$\Pi_{AB}(q^2 << \Lambda^2) = \Pi_{AB}(0) + q^2 \Pi'_{AB}(0) + \frac{(q^2)^2}{2}\Pi''_{AB}(0) + \cdots$$

Hence, once again, the functions $\Pi_{AB}(q^2)$ are reduced, to 7 numbers, which we call S, T, U, V, W, X, Y. For simplicity, we truncate to $O(q^2)$ and thus, have only 3 parameters S, T, U.

We have,

$$\begin{aligned}
\alpha T &= \frac{\Pi_{WW}(0)}{m_W^2} - \frac{\Pi_{ZZ}(0)}{m_Z^2} \\
\frac{\alpha S}{\sin^2 2\theta} &= \Pi'_{ZZ}(0) - \frac{2\cos 2\theta}{\sin 2\theta}\Pi'_{Z\gamma}(0) - \Pi'_{\gamma\gamma}(0) \\
\frac{\alpha U}{4\sin^2\theta} &= \Pi'_{WW}(0) - \cos^2\theta\,\Pi'_{ZZ}(0) \\
&\quad - \sin 2\theta\,\Pi'_{\gamma Z}(0) - \sin^2\theta\,\Pi'_{\gamma\gamma}(0)
\end{aligned}$$

Now, we can write the differences between the mixing angles as follows:

$$\begin{aligned}
\sin^2\theta_* - \sin^2\theta_0 &= \frac{\alpha}{4\cos 2\theta}(S - \sin^2 2\theta\, T) \\
\sin^2\theta_0 - \sin^2\theta_W &= \frac{\alpha\cos^2\theta}{\cos 2\theta}\left(-\frac{1}{2}S - \cos^2\theta\, T + \frac{\cos 2\theta}{4\sin^2\theta}U\right)
\end{aligned}$$

Experimentally, we have

$$\begin{aligned}
S - S_{SM} &= +0.00 \pm 0.07 \\
T - T_{SM} &= +0.05 \pm 0.06
\end{aligned}$$

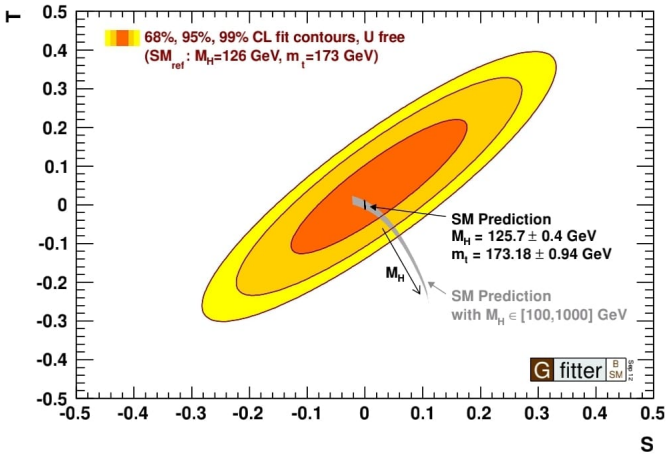

The scale at which EWPMs can probe BSM is upto 2 orders of magnitude above the weak scale, because EWPMs have an accuracy of the order of 10% of the SM 1-loop corrections:

$$\frac{\Lambda}{\sqrt{|c_{WB}|}} > 14\ TeV\sqrt{\frac{0.07}{|S|}}$$

$$\frac{\Lambda}{\sqrt{|c_{HH}|}} > 6\ TeV\sqrt{\frac{0.11}{|T|}}$$

4 Experimental Aspects

4.1 Indirect measurements of the top and the Higgs mass

First, we list out the experimentally measured values of the electroweak parameters:

$$1/\alpha(0) = 137.0359895(61) \text{ (Quantum hall effect and g-2 of the electron)}$$
$$G_F = 1.166389(22) \times 10^{-5}\ GeV^{-2} \text{ (muon decay)}$$
$$M_Z = 91.1867(20)\ GeV \text{ (direct measurement from decay width)}$$

In addition, QCD corrections to observables will depend on

$$\alpha_s(M_Z^2) = 0.1192 \pm 0.0020$$

Now we analyze how these parameters help in top/Higgs mass measurement. We take any observable O that depends on $(\alpha, G_F, M_Z, \alpha_s)$, and on m_t, M_H:

$$O_{th} = f(\alpha, G_F, M_Z, \alpha_s; m_t, M_H).$$

We measure O and compare with theory to get:

$$O_{exp} = O_{th} \equiv f(\alpha, G_F, M_Z, \alpha_s; m_t, M_H).$$

This puts constraints on the allowed values of m_t and M_H!

We must repeat this procedure for all observables to check for consistency.

We assume the Higgs mass to be 300 GeV within the range 70 GeV to 1 TeV. Then one gets

$$m_t = (177 \pm 7^{+16}_{-19}) GeV,$$

the super(sub)scripts denoting errors from the uncertainty in the assumed Higgs mass.

This is comparable to the direct measurement at Fermilab:

$$m_t = 175.6 \pm 5.5 \ GeV.$$

Below, we show the progress made in measuring the top mass over the years.

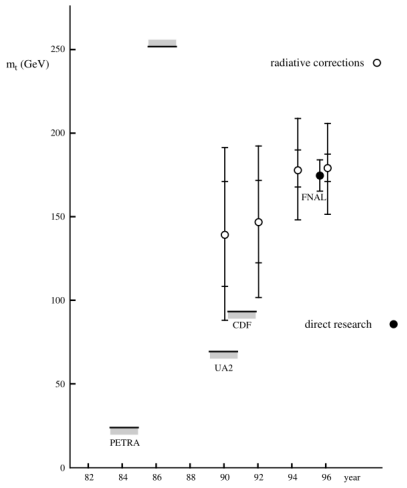

Figure 2: Progress in determination of the top mass

EWPMs constrain the allowed range in the $m_t - M_H$ plane as follows:

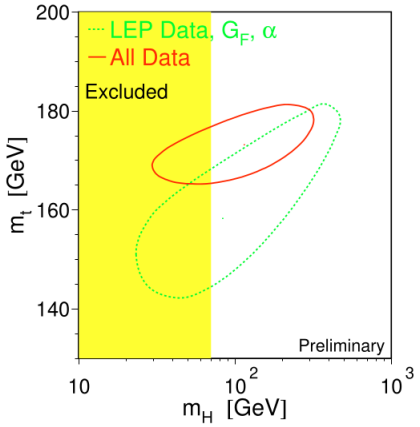

Figure 3: Experimentally allowed region for top and Higgs masses

4.2 Precision experiments at LEP

We start by analyzing cross-sections as observables for EWPM. For a massive gauge boson at a higher loop order, the propagator acquires an imaginary part:

$$\frac{i}{(p^2 - M^2) + iM\Gamma}$$

In the rest frame, this results in a particle resonance proportional to

$$\frac{1}{(E^2 - M^2) + iM\Gamma}$$

The corresponding probability distribution will be a Breit-Wigner distribution:

$$f(E) = \frac{k}{(E^2 - M^2)^2 + M^2\Gamma^2}$$

where, Γ =the decay width, which is the width at half-maximum of the distribution.
$(f(E) \to 2M\delta(E^2 - M^2)$ as $\Gamma \to 0)$

The EW cross section for e^-e^+ annihilation is given by

$$\frac{2s}{\pi}\frac{1}{N_c^f}\frac{d\sigma_{\text{ew}}}{d\cos\theta}\left(e^+e^- \to f\bar{f}\right) = \alpha^2(s)\left[F_1(1+\cos^2\theta) + 2F_2\cos\theta\right] + B$$

where

$$\begin{aligned}
F_1 &= Q_e^2 Q_f^2 \chi Q_e Q_f g_V^e g_V^f \cos\delta_R + \chi^2\left((g_V^e)^2 + (g_A^e)^2\right)\left((g_V^f)^2 + (g_A^f)^2\right)\\
F_2 &= -2\chi Q_e Q_f g_A^e g_A^f \cos\delta_R + 4\chi^2 g_V^e g_A^e g_V^f g_A^f,\\
\tan\delta_R &= M_Z\Gamma_Z/(M_Z^2 - s),\\
\chi(s) &= \frac{G_F s M_Z^2}{2\sqrt{2}\pi\alpha(s)\left[(s - M_Z^2)^2 + \Gamma_Z^2 M_Z^2\right]^{1/2}},
\end{aligned}$$

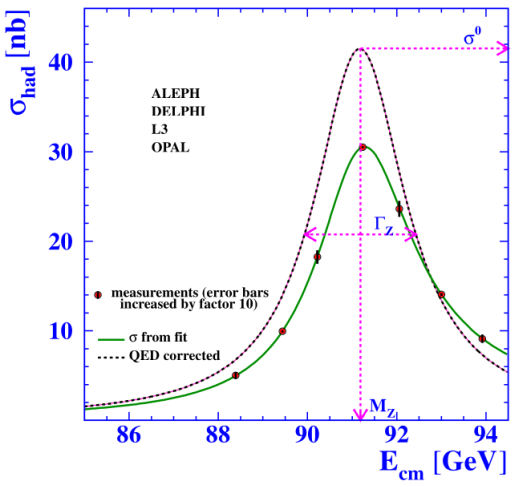

Define:

$$A_f = \frac{2g_A^f/g_V^f}{1+(g_A^f/g_V^f)^2}$$

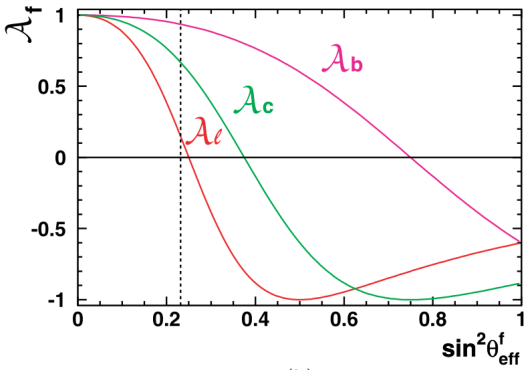

$$A_{FB} = \frac{\sigma_F - \sigma_B}{\sigma_F + \sigma_B} = \frac{3A_e}{4A_f}$$

$$A_{LR} = \frac{\sigma_L - \sigma_R}{\sigma_L + \sigma_R} = A_e$$

$$\gamma_f = \frac{\sum_f((g_V)^2 + (g_A)^2)}{\Sigma_{\rm tot}}$$

Table 1 Z branching ratios for $x = \sin^2\theta_W = 0.2315$.

Particles Symbol	Couplings (Eq. (4))			Branching ratios	
	g_V	g_A	$\sum(g_V^2+g_A^2)$	calc.	obs.
ν_e,ν_μ,ν_τ	$\frac{1}{2}$	$\frac{1}{2}$	$3(\frac{1}{2})^2+3(\frac{1}{2})^2$	20.5%	$20.00\pm0.06\%$
e,μ,τ	$-\frac{1}{2}+2x$	$-\frac{1}{2}$	$3(-\frac{1}{2}+2x)^2+3(\frac{1}{2})^2$	10.3%	$10.097\pm0.0069\%$
u,c	$\frac{1}{2}-\frac{4}{3}x$	$\frac{1}{2}$	$6(\frac{1}{2}-\frac{4}{3}x)^2+6(\frac{1}{2})^2$	23.6%	$23.2\pm1.2\%$
d,s	$-\frac{1}{2}+\frac{2}{3}x$	$-\frac{1}{2}$	$6(-\frac{1}{2}+\frac{2}{3}x)^2+6(\frac{1}{2})^2$	30.3%	$31.68\pm0.8\%$
b	$-\frac{1}{2}+\frac{4}{3}x$	$-\frac{1}{2}$	$3(-\frac{1}{2}+\frac{2}{3}x)^2+3(\frac{1}{2})^2$	15.3%	$15.12\pm0.05\%$

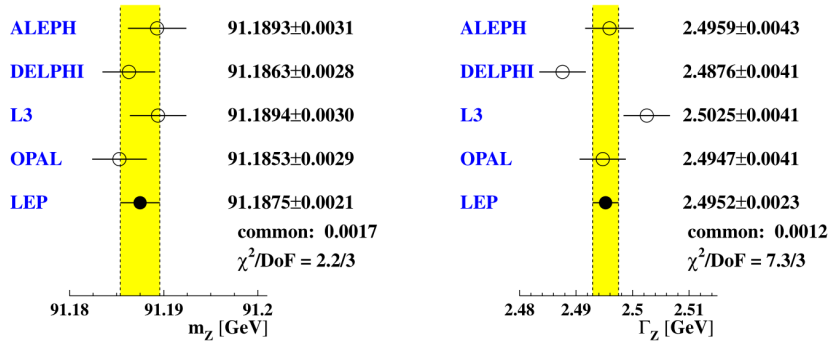

4.3 Experimental precision of EWPMs

The experimentally observed total cross-section is

$$\sigma_{tot} = \frac{N_{sel} - N_{bg}}{\epsilon_{sel}\mathcal{L}}$$

We briefly discuss errors introduced due to the factors $N_{bg}/N_{sel}, \epsilon_{sel}$ and $\mathcal{L}$.

The combination of magnetic spectrometers with good tracking, electromagnetic and hadronic calorimeters and muon tracking allows a good discrimination of $q\bar{q}$ from l^+l^- final states and a strong reduction of background, which was typically below 1% for all final states.

The factor ϵ_{sel} includes geometrical acceptance as well as the selection efficiency. For muon trackers, a typical geometrical acceptance is $|\cos\theta| \leq 0.9$ and selection efficiency is $> 95\%$.

The luminosity is determined from small angle Bhabha scattering using the acceptance calculations and cross-section from the BHLUMI Monte-Carlo event generator, which was used by all experiments leading to a correlated common error from the higher order uncertainties in the Bhabha scattering cross-section of 0.061%.

This *common correlated* uncertainty corresponds to the luminosity process $e^+e^- \rightarrow e^+e^- + (n)\ \gamma$ at $O(\alpha^2)$ level, in the context of Yennie-Frautschi-Suura exponentiation.

In all of the following discussion, χ^2 analysis has been used for curve fitting.

5 Constraints on the Standard Model

5.1 Constraints on the SM before the Higgs

We were able to write relations among observables at the tree level using 3 EW parameters. Taking into account loop corrections, we expand the set of relevant parameters to $m_Z, m_t, M_H, \alpha_s, \Delta\alpha^{(5)}_{had}(m_Z)$. We exclude G_F from this discussion as it is already very precisely known. ($\Delta\alpha^{(5)}_{had}(m_Z)$ is the hadronic contribution to the running of the fine structure constant at m_Z.)

From a fit to the Z-pole data and preliminary data for m_t and m_W the EWWG finds for these

parameters:

$$m_Z = 91.1874 \pm 0.0021$$
$$m_t = 178.5 \pm 3.9 GeV$$
$$M_H = 129^{+74}_{-49} GeV$$
$$\alpha_s = 0.1188 \pm 0.0027$$
$$\Delta\alpha^{(5)}_{had}(m_Z) = 0.02767 \pm 0.00034$$

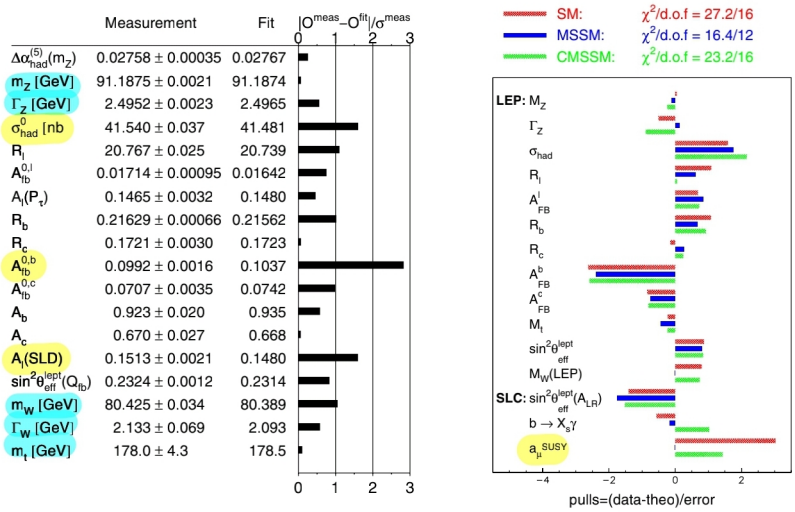

Figure 4: Theoretical predictions vs Experimentally measured values for various observables and differences marked in number of standard deviations.

In particular, we notice that the magnetic moment of the muon is predicted very precisely bu the MSSM(Minimal Supersymmetric extension of Standard Model) over the erroneous SM prediction.

5.2 Constraints on the SM after the Higgs

We present the allowed regions in $m_W - m_t$ planes,before and after the discovery of the Higgs:

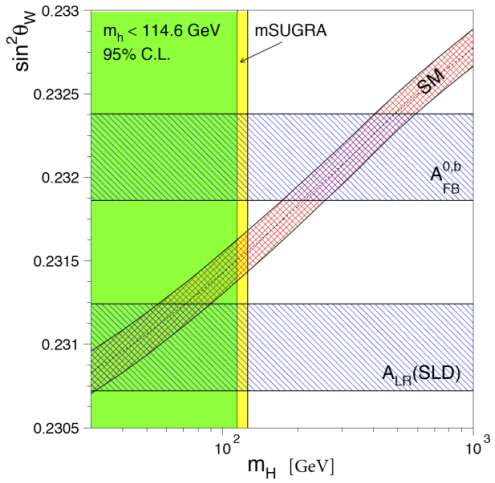

Figure 5: Allowed region in the $\theta_W - m_H$ plane; the green region is forbidden by prior LEP data

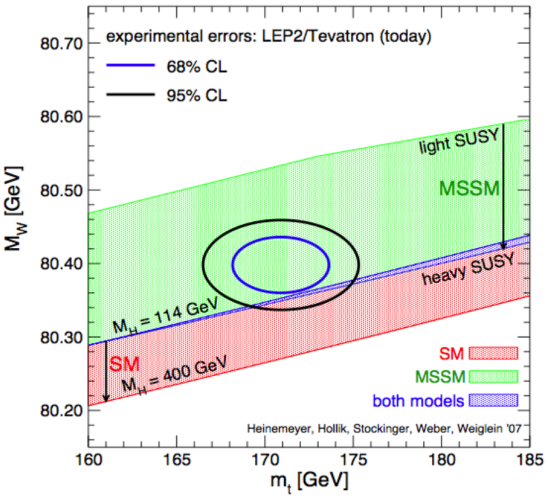

(a) BEFORE

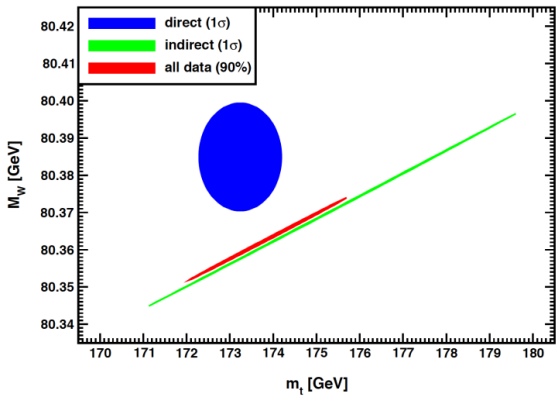

(b) AFTER

The value of the directly measured m_W is 1.5σ above the SM prediction, which implies some tension between m_W and M_H , since lower values of M_H would shift the SM prediction of m_W upwards.

Allowed range in the $M_H - m_t$ plane, after the discovery of the Higgs:

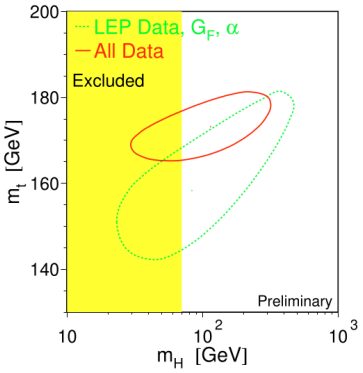

(a) BEFORE

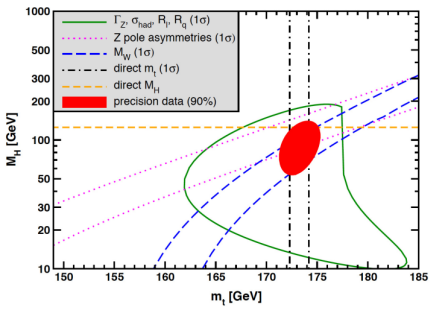

(b) AFTER

The central value of the ellipse (indirect measurements) in the second figure is slightly below the direct measurement of the Higgs boson mass, since the slightly high value of m_W pulls the Higgs mass to lower values.

6 Discrepancy in W mass

Tevatron at FermiLab is a $p\bar{p}$ collider that shut down on September 29, 2011. Its data (CDF II) was analyzed upto 2022, and it was found that it showed a W mass incompatible with the SM expectations.

We will take as our parameters for EWPMs, the following:

- $\alpha^{-1}(m_Z) = 127.918(18)$
- $G_F = 1.16637(1) \times 10^{-5}\ GeV^{-2}$
- $m_Z = 91.1876(21)\ GeV$
- $m_t = 172.89(59)\ GeV$
- $M_H = 125.25(17)\ GeV$

With these measured values, the SM expectation for the W mass is:

$$m_W = (80357 \pm 4(inputs) \pm 4(theory))\ MeV$$

Now we take a look at the experimental results.

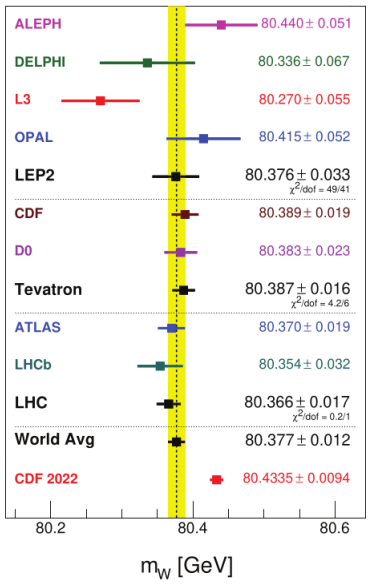

In the first run of the CDF, FermiLab produced data at a luminosity of 2.2 fb^{-1} and the results for the W mass were in agreement with SM. Later, in the CDF II run, with a much higher luminosity of 8.8 fb^{-1}, the new results had a much lower uncertainty due to the high luminosity. However, the measured value was outside SM expectations by 7 standard deviations. A 7σ tension is well beyond the usual discovery threshold of 5σ in particle physics. This implies either *new physics* or *experimental error*.

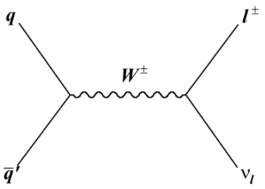

The measurements are performed in the $\mu\nu_\mu$ and $e\nu_e$ channels using 200pb^{-1} (350pb^{-1}) for M_W (Γ_W)

$$m_T = \sqrt{2 p_T^{\,l} p_T^{\,\nu} (1 - \cos\phi_{l\nu})}$$

μ-channel: central tracker
e-channel: EM calorimeter

inferred from missing transverse energy

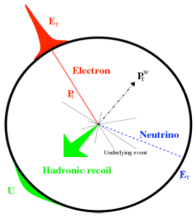

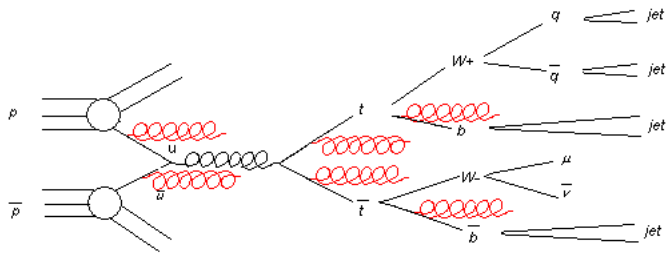

Figure 8: Measuring W bosons through νl production in $p\bar{p}$ collisions

* * * *

Aside: CDF experiment at Tevatron

The Fermilab Tevatron produced high yields of W bosons from 2002 to 2021 through quark-antiquark annihilation in collisions of protons and antiprotons at the CM energy 1.96 TeV. The (anti)quark momentum distributions in the (anti)proton are the best measured among all constituent partons of colliding particles. The use of proton-antiproton collisions reduces uncertainties on the momenta of partons and the corresponding W boson mass, where W bosons are produced from quarks or antiquarks and gluons, the latter of which have less precisely known momentum distributions.
The data sample corresponds to an integrated luminosity of 8.8 fb^{-1} of $p\bar{p}$ collisions collected by the CDF II detector.

In the cylindrical detector, trajectories of charged particles (tracks) produced in the collisions are measured by means of a wire drift chamber (a central outer tracking drift chamber, or COT) immersed in a 1.4 T axial magnetic field.

The W boson mass is inferred from the kinematic distributions of the decay leptons (l). Because the neutrino from the W boson decay is not directly detectable, its transverse momentum p_T^ν is deduced by imposing transverse momentum conservation. Longitudinal momentum balance cannot be imposed because most of the beam momenta are carried away by collision products that remain close to the beam axis, outside the instrumented regions of the detector. By design of the detector, such products have small transverse momentum. The transverse momentum vector sum of all detectable collision products accompanying the W or Z boson is defined as the hadronic recoil, where the sum is performed over calorimeter towers. Calorimeter towers containing energy deposition from the charged lepton(s) are excluded from this sum.

In analogy with a 2-body mass, the W boson transverse mass is defined using only transverse momentum vectors as

$$m_T = \sqrt{2p_T^l p_T^\nu (1 - \cos\phi_{l\nu})}$$

* * * *

We briefly mention various possible reasons for this discrepancy.

- Supersymmetry: Superpartners of quarks (squarks) could contribute to loop corrections to the W propagator.

- Extension of the Higgs sector: Additional Higgs doublets do not change the gauge boson masses at tree level, but they CAN do so at loop level. Singlet extensions of the Higgs (i.e. SM + real singlet scalar) can alter the gauge boson mass. Triplet Higgs extensions will break custodial symmetry of the Higgs potential, thus affecting $\sin^2\theta_W$, and, hence, m_W.
- BSM gauge bosons
- Hypothetical sources of dark matter

We conclude this section by noting that the the recent results by CMS (*High-precision measurement of the W boson mass with the CMS experiment at the LHC*, 18 December 2024) at luminosity 16.8 fb^{-1} resolve this controversy, and show that the W mass is within the SM expected value:

$$m_W = 80360.2 \pm 9.9 MeV$$

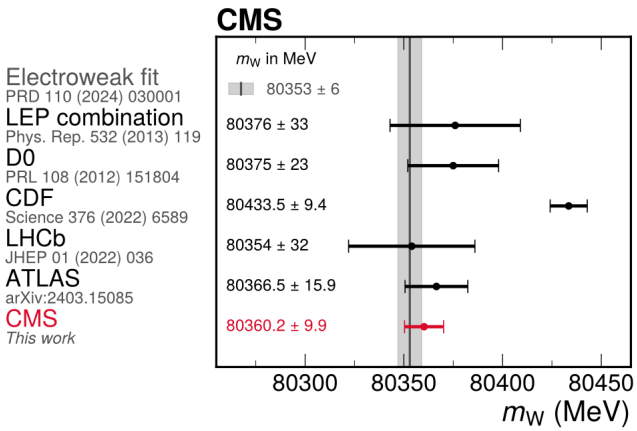

References

[1] The Standard Model: From Fundamental Symmetries to Experimental Tests, Grossman and Nir.

[2] Lepton Universality, Michel Davier.

[3] Precision experiments at LEP, W. de Boer.

[4] DOE HEP Closeout Report, Ashutosh Kotwal, Duke University

[5] High-precision measurement of the W boson mass with the CMS experiment at the LHC, the CMS Collaboration. arXiv:2412.13872v1.